Biomedical Research and Therapy 2026, 13(08):8965-8979

Open Access Full Text Article

Original Research

Human Dental Pulp–Derived Mesenchymal Stem Cells Improve Ovarian Function Through Modulation of Wnt/β-Catenin Signaling in a Cyclophosphamide-Induced Premature Ovarian Failure Rat Model

Münevver Senen[1], Nazli Cil[2,*], Cihan Kabukcu[3], Hande Senol[4], Ergun Mete[5], Gülçin Abban Mete[2]

[1]*Department of Hematology at Kayseri City Training and Research Hospital, Kayseri City Hospital, Kocasinan, Turkey*

[2]*Department of Histology and Embryology, Faculty of Medicine, Pamukkale University, Pamukkale, Denizli, Turkey*

[3]*Department of Obstetrics and Gynecology, Faculty of Medicine, Pamukkale University, Pamukkale, Denizli, Turkey*

[4]*Department of Biostatistics, Faculty of Medicine, Pamukkale University, Pamukkale, Denizli, Turkey*

[5]*Department of Microbiology, Faculty of Medicine, Pamukkale University, Pamukkale, Denizli, Turkey*

Correspondence

Nazli Cil, Department of Histology and Embryology, Faculty of Medicine, Pamukkale University, Pamukkale, Denizli, Turkey

Email: ncil@pau.edu.tr

History

- Received: Jun 19, 2026
- Accepted: Aug 02, 2026
- Published Online: Aug 31, 2026

DOI : 10.15419/bmrat.v13i8.1099

ABSTRACT

Background: Premature ovarian failure (POF) is a debilitating complication of cytotoxic chemotherapy, characterized by the accelerated depletion of the ovarian primordial follicle reserve and the consequent loss of endocrine and reproductive function. Mesenchymal stem cell (MSC) transplantation has emerged as a promising cytoprotective and regenerative modality; however, the precise molecular mechanisms governing MSC-mediated ovarian recovery remain incompletely understood. This study aimed to investigate the therapeutic efficacy of human dental pulp–derived mesenchymal stem cells (DP-MSCs) in preserving ovarian structural architecture and follicular reserve in a cyclophosphamide (CTX)-induced POF rat model, with a specific focus on the canonical Wnt/β-catenin signaling pathway. **Methods:** Female Wistar albino rats were randomly allocated into four experimental groups (n = 8 per group): Control, Sham (saline), POF, and DP-MSC. POF was induced via an initial intraperitoneal injection of CTX (200 mg/kg) on day 1 followed by daily maintenance injections of 8 mg/kg/day for 14 consecutive days. On day 15, animals in the treatment group received a local intraovarian injection of 2×10^6 human DP-MSCs suspended in phosphate-buffered saline. Ovarian function and morphology were evaluated 10 days post-transplantation via serum hormonal profiling (anti-Müllerian hormone [AMH], follicle-stimulating hormone [FSH], and luteinizing hormone [LH]), differential follicle counting, histopathological examination, and semi-quantitative immunohistochemical analysis of Wnt-1, Wnt-4, and β-catenin expression. **Results:** CTX administration caused extensive follicular depletion across all developmental stages, significant stromal fibrosis, increased follicular atresia, and dysregulated LH secretion. Local DP-MSC transplantation effectively mitigated these cytotoxic damages, significantly increasing primordial, secondary, and tertiary (antral) follicle counts, restoring functional corpora lutea, and markedly decreasing atretic and cystic follicle numbers ($p < 0.05$). Immunohistochemical analysis revealed that DP-MSC transplantation preserved prominent Wnt-1 immunoreactivity in primordial follicles and successfully restored Wnt-4 expression in primary follicles and corpora lutea, which was largely lost in untreated POF ovaries. Stable cytoplasmic and nuclear β-catenin expression was observed across all groups, confirming the presence of active canonical signaling machinery. **Conclusion:** Local intraovarian transplantation of human DP-MSCs effectively preserves the primordial follicle pool and restores ovarian histological architecture in CTX-induced POF rats. These therapeutic benefits appear to be mediated, at least in part, through the reactivation and modulation of the canonical Wnt/β-catenin signaling pathway, particularly via the restoration of Wnt-4 expression. DP-MSCs represent a viable, accessible, and potent candidate for stem cell-based ovarian regenerative therapies.

Key words: Cyclophosphamide, Premature ovarian failure, Dental pulp stem cells, Mesenchymal stem cell transplantation, Folliculogenesis, Wnt/β-catenin signaling pathway

INTRODUCTION

Premature ovarian failure (POF), also referred to as primary ovarian insufficiency (POI), is a major cause of female infertility characterized by the premature cessation of normal ovarian function before the age of 40 years[1]. Pathophysiologically, POF is defined by the accelerated depletion of the quiescent primordial follicle pool, amenorrhea, hypoestrogenism, and elevated serum gonadotropin levels[1,2]. Histologically, chemotherapy-induced POF manifests as extensive ovarian parenchymal atrophy, interstitial stromal fibrosis, microvascular degeneration, and marked follicular atresia, accompanied by severe disruption of normal folliculogenesis[2]. Conventional therapeutic approaches, primar-

Cite this article : Senen M, Cil N, Kabukcu C, Senol H, Mete E, Mete GA. **Human Dental Pulp–Derived Mesenchymal Stem Cells Improve Ovarian Function Through Modulation of Wnt/β-Catenin Signaling in a Cyclophosphamide-Induced Premature Ovarian Failure Rat Model**. *Biomed. Res. Ther.* 2026; 13(08):8965-8979.

ily hormone replacement therapy (HRT), are limited to alleviating hypoestrogenic symptoms; they fail to restore biological ovarian function or rescue the depleted follicular reserve, highlighting the urgent need for novel regenerative therapeutic strategies[3]. Mesenchymal stem cells (MSCs) have emerged as highly promising candidates for regenerative medicine owing to their self-renewal capacity, multilineage differentiation potential, and robust immunomodulatory and paracrine secretome profiles[4,5]. Preclinical studies have demonstrated that MSC transplantation can promote ovarian tissue repair, attenuate granulosa cell apoptosis, stimulate local neo-angiogenesis, and potentially support germ cell lineage maintenance under favorable microenvironmental conditions[4,5]. Among the various tissue sources available, dental pulp–derived mesenchymal stem cells (DP-MSCs) have garnered particular interest. DP-MSCs originate from the embryonic neural crest, are readily accessible from discarded permanent third molars or deciduous teeth without invasive harvesting procedures, and exhibit superior proliferation rates, genomic stability, and strong neurovascular and regenerative properties compared to conventional bone marrow–derived MSCs (BM-MSCs)[6,7].

The molecular cascades driving stem cell-mediated ovarian regeneration are multifaceted, with developmental signaling pathways playing pivotal regulatory roles. In particular, the Wnt signaling cascade represents an evolutionarily conserved network essential for embryogenesis, organogenesis, tissue homeostasis, and cellular fate determination. It coordinates essential biological processes, including cell proliferation, survival, polarity, and migration, which are vital for maintaining structural integrity and orchestrating tissue repair[8]. Within the female reproductive system, canonical Wnt/β-catenin signaling is indispensable for gonadal differentiation and ovarian development[8,9]. Experimental studies have established that Wnt-4 is an absolute requirement for normal female sex determination and folliculogenesis; mice lacking Wnt-4 exhibit severe ovarian dysgenesis and a drastically depleted follicular pool[9]. Furthermore, Wnt-1 has been reported to stimulate granulosa cell proliferation and suppress apoptosis via activation of the canonical Wnt/β-catenin pathway, underscoring its key role in early follicular maturation[8].

Beyond its structural roles, the canonical Wnt/β-catenin pathway is intricately involved in the regulation of ovarian steroidogenesis. Wnt signaling actively crosstalks with gonadotropin signaling pathways to modulate target gene transcription regulated by follicle-stimulating hormone (FSH) and luteinizing hormone (LH)[10]. Consequently, perturbation or suppression of this signaling cascade compromises granulosa cell viability, impairs follicular maturation, and contributes to the pathogenesis of POF.

Therefore, this study aimed to investigate the therapeutic effects of human DP-MSCs on ovarian histological architecture and follicular reserve in a cyclophosphamide (CTX)-induced POF rat model, with a specific focus on the modulation of the canonical Wnt/β-catenin signaling pathway.

MATERIALS AND METHODS

Animals and Experimental Design

This study was conducted in accordance with international guidelines for the care and use of laboratory animals and was approved by the Pamukkale University Animal Experiments Ethics Committee (Approval No. PAUHDEK-2021/38). A total of 32 adult female Wistar albino rats (weighing 250–350 g) were housed under controlled standard laboratory conditions (temperature: 21 ± 1 ℃, relative humidity: 65–70%, 12-hour light/dark cycle) with ad libitum access to standard rodent chow and water.

The animals were randomly allocated into four experimental groups (n = 8 per group):

1. **Control group:** received no interventions or injections throughout the study period.
2. **Sham group:** received daily intraperitoneal (i.p.) injections of physiological saline (0.9% NaCl) for 14 consecutive days.
3. **POF group:** premature ovarian failure was induced via an initial loading i.p. injection of CTX (200 mg/kg; Sigma-Aldrich, St. Louis, MO, USA) on day 1, followed by daily maintenance i.p. injections of 8 mg/kg/day for 14 consecutive days.
4. **DP-MSC group:** following the 14-day CTX regimen as described above, animals received a local intraovarian injection of 2×10^6 human DP-MSCs suspended in 0.2 mL phosphate-buffered saline (PBS) on day 15, administered bilaterally using a 1-mL insulin syringe equipped with a 26-gauge needle under aseptic conditions.

On day 25 (10 days post-transplantation), all animals were deeply anesthetized and euthanized. Blood samples were collected via cardiac puncture for biochemical analysis, and ovaries were harvested and processed for histological and immunohistochemical evaluations.

DP-MSC Isolation, Culture, and Characterization

Human DP-MSCs were isolated from healthy impacted third molars following approval from the Pamukkale University Non-Interventional Clinical Research Ethics Committee (Approval No. 17, dated July 8, 2020) and informed donor consent. Cells at passage 3 were maintained in Dulbecco's Modified Eagle Medium (DMEM; Gibco, Grand Island, NY, USA) supplemented with 10% fetal bovine serum (FBS; Gibco) and 1% penicillin–streptomycin at 37 ℃ in a humidified incubator containing 5% CO_2.

The immunophenotypic profile of DP-MSCs was verified by flow cytometry using monoclonal antibodies against human CD73, CD90, and CD34 (Beckman Coulter, Brea, CA, USA). Trilineage multipotency was validated by culturing cells in osteogenic, adipogenic, and chondrogenic differentiation media for 21 days, followed by specific staining with Alizarin Red S (calcium deposits), Oil Red O (neutral lipid vacuoles), and Alcian Blue (sulfated glycosaminoglycans), respectively.

Hormonal Analysis

Blood samples were collected via cardiac puncture under deep anesthesia, allowed to clot for 30 minutes at room temperature, and centrifuged at 3,000 × g for 15 minutes at 4 ℃. Serum was separated and stored at −80 ℃ until analysis. Serum concentrations of AMH, FSH, and LH were measured using rat-specific enzyme-linked immunosorbent assay (ELISA) kits (Bioassay Technology Laboratory [BT LAB], Shanghai, China) according to the manufacturer's instructions. All samples were analyzed in duplicate. Optical density was measured at 450 nm using a microplate reader (BioTek ELx800; BioTek Instruments Inc., Winooski, VT, USA), and absolute hormone concentrations were calculated using standard calibration curves.

Histological Evaluation and Differential Follicle Counting

Excised ovarian tissues were fixed in 10% neutral buffered formalin for 24 hours, dehydrated through an ascending ethanol series, cleared in xylene, and embedded in paraffin wax. Serial sections (5-µm thickness) were prepared and stained with hematoxylin and eosin (H&E) for structural evaluation.

For quantitative follicle counting, every 5th section (specifically the 1st, 5th, and 10th sections per ovary) was systematically selected to avoid double counting. Only follicles containing an oocyte with an identifiable nucleus were counted and classified according to standard morphological criteria [11,12]:

- **Primordial follicles:** an oocyte surrounded by a single layer of flattened, squamous pregranulosa cells;
- **Primary follicles:** an oocyte surrounded by a single layer of cuboidal granulosa cells;
- **Secondary follicles:** an oocyte enclosed by two or more layers of cuboidal granulosa cells without an antral cavity;
- **Tertiary (antral) follicles:** a follicle exhibiting a well-defined, fluid-filled antral cavity;
- **Atretic follicles:** follicles displaying apoptotic/pyknotic granulosa cells, cellular detachment from the basement membrane, or degenerated oocytes;
- **Cystic follicles** and **corpora lutea** were also quantified across sections.

All microscopic examinations were performed using an Olympus BX53 light microscope by two independent histologists blinded to the study groups.

Immunohistochemical Analysis

Paraffin sections (5-µm thickness) were deparaffinized in xylene and rehydrated through a descending graded ethanol series. Heat-induced antigen retrieval was performed in 10 mM citrate buffer (pH 6.0) using a microwave oven, followed by cooling to room temperature. Endogenous peroxidase activity was blocked with 3% hydrogen peroxide in methanol for 10 minutes. Non-specific binding was blocked using a protein blocking solution (ScyTek Laboratories, Logan, UT, USA).

Sections were incubated overnight at 4 ℃ with primary rabbit polyclonal antibodies against Wnt-1 (1:300; Bioss Antibodies, Woburn, MA, USA), Wnt-4 (1:300; Bioss Antibodies), and β-catenin (1:300; Bioss Antibodies). After PBS washes, sections were incubated with a biotinylated secondary antibody, followed by streptavidin–horseradish peroxidase conjugate (ScyTek Laboratories). Immunoreactivity was visualized using 3,3′-diaminobenzidine (DAB) as the chromogen substrate. Sections were counterstained with Mayer's hematoxylin, dehydrated, cleared, and mounted. Negative controls were prepared by omitting the primary antibody. Immunoreactivity was evaluated semi-quantitatively based on staining intensity as negative (–), weak (+), moderate (++), or strong (+++) by two blinded observers.

Statistical Analysis

Statistical analyses were performed using IBM SPSS Statistics for Windows, Version 25.0 (IBM Corp., Armonk, NY, USA). Continuous variables were expressed as mean ± standard deviation (SD) for normally distributed data or as median with interquartile range (IQR; 25th–75th percentiles) for non-normally distributed data. Normality was evaluated using the Shapiro–Wilk test. Differences among multiple independent groups were analyzed using one-way analysis of variance (ANOVA) followed by Tukey's post hoc test for normally distributed parameters, or the Kruskal–Wallis test followed by post hoc pairwise Mann–Whitney U tests with Bonferroni correction for non-normally distributed variables. All statistical tests were two-tailed, and a p-value < 0.05 was considered statistically significant.

RESULTS

Phenotypic and Functional Characterization of Human DP-MSCs

Flow cytometric immunophenotyping confirmed the characteristic mesenchymal surface profile of isolated human DP-MSCs. The cells demonstrated strong positive surface expression of characteristic mesenchymal markers CD73 (99.92%) and CD90 (96.76%), alongside negligible expression of the hematopoietic lineage marker CD34 (0.08%) (Figure 1, Panel I). Under phase-contrast microscopy, passage 3 DP-MSCs displayed typical spindle-shaped, fibroblast-like morphology with plastic-adherent growth (Figure 1, Panel IIA). Multilineage differentiation potential was verified by successful differentiation into adipocytes (Oil Red O-positive neutral lipid droplets; Figure 1, Panel IIB), osteo-

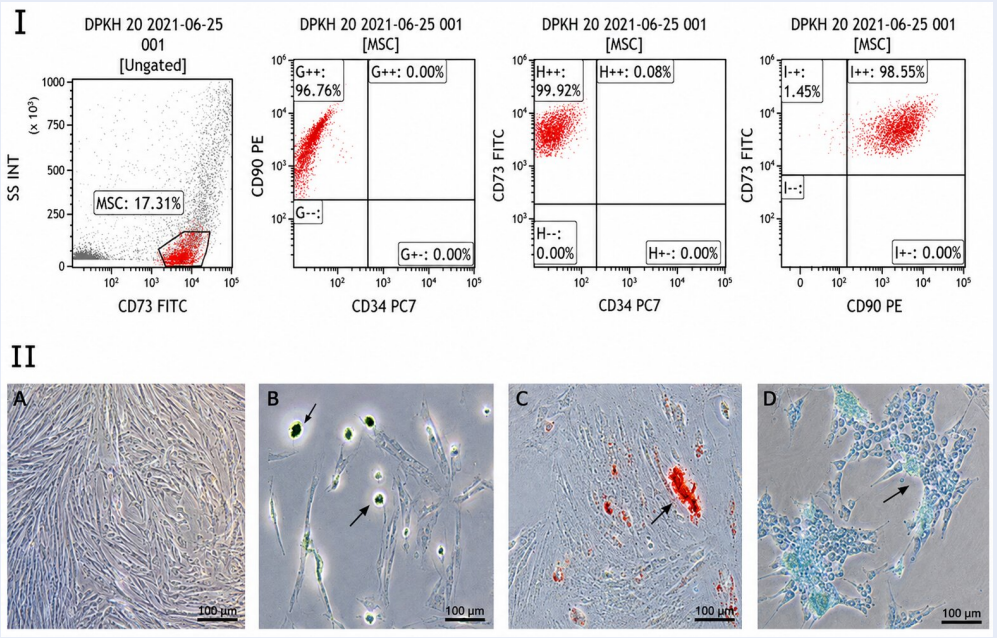

Figure 1: **Phenotypic characterization and multilineage differentiation potential of human dental pulp–derived mesenchymal stem cells (DP-MSCs). (I)** Flow cytometric immunophenotyping of passage 3 DP-MSCs demonstrating strong positive surface expression of characteristic mesenchymal markers CD90 (96.76%) and CD73 (99.92%), alongside negligible expression of the hematopoietic lineage marker CD34 (0.08%). Gates were set using appropriate isotype controls. **(II)** Morphological appearance and in vitro trilineage differentiation assays: **(A)** Phase-contrast microscopy showing passage 3 DP-MSCs exhibiting characteristic spindle-shaped, fibroblast-like morphology with plastic adherence (arrows); **(B)** Adipogenic differentiation verified by Oil Red O staining of intracellular neutral lipid droplets (arrows) following 21 days of adipogenic induction; **(C)** Osteogenic differentiation confirmed by Alizarin Red S staining of mineralized calcium nodules (arrow) following 21 days of osteogenic induction; **(D)** Chondrogenic differentiation confirmed by Alcian Blue staining of sulfated proteoglycans within the extracellular matrix (arrows) following 21 days of chondrogenic induction. Micrographs were acquired using an inverted phase-contrast microscope at 200× total magnification (20× objective). **Abbreviations:** CD, cluster of differentiation; DP-MSC, dental pulp–derived mesenchymal stem cell; FITC, fluorescein isothiocyanate; PE, phycoerythrin; PC7, phycoerythrin-cyanine 7; SS INT, side scatter intensity.

Table 1: Comparison of initial weights, final weights, and changes in body weight for each group.

		Initial weight (gr)	Final weight (gr)	Changes in body weight
Control	A.M. ± S.D	260.8±43.45	288.6±20.44	27.8±35.18
	Med (IQR)	273 (219.5-296)	296 (267.5-306)	35 (-6.5-58.5)
	min - max	192-297	260-308	22-68
Sham	A.M. ± S.D	258.43±7.98	277.43±9.2	19±7.81 (b)
	Med (IQR)	255 (253-265)	277 (268-286)	19 (13-24)
	min – max	249-271	265-290	9-33
POF	A.M. ± S.D	256±12.43	268.33±12.08	12.33±9.5
	Med (IQR)	250 (245-266)	270 (259-281)	12 (4-18.5)
	min – max	244-279	248-283	4-31
DP-MSC	A.M. ± S.D	262.1±12.91	265±14.93 (a)	2.9±15.41
	Med (IQR)	260 (252-268.5)	262 (257.5-272.5)	-2.5 (-5-10)
	min – max	247-292	245-292	-13-42
Intergroup p-value		0.583(kw=1.94)	0.024* (F=3.673)	0.029* (kw=9.046)

*p<0.05 A.M: Arithmetic mean, S.D: Standard deviation, Med (IQR): Median (25th-75th percentiles), min – max: Minimum and maximum values, F: One-Way Analysis of Variance, kw: Kruskal-Wallis Analysis of Variance, a: Significant difference versus the control group; b: Significant difference versus the POF group.

cytes (Alizarin Red S-positive mineralized calcium nodules; Figure 1, Panel IIC), and chondrocytes (Alcian Blue-positive sulfated proteoglycans; Figure 1, Panel IID). Together, these phenotypic and functional assays confirmed the MSC identity of the isolated cell populations.

Body Weight Changes

At baseline, initial body weights did not differ significantly among the experimental groups (p = 0.583; Table 1). At the end of the experimental period, a statistically significant difference in final body weight was observed across groups (F = 3.673, p = 0.024), with the Control group exhibiting significantly higher final weights (288.60 ± 20.44 g) compared to the DP-MSC group (265.00 ± 14.93 g; p < 0.05). Furthermore, net body weight gain differed significantly among the groups (Kruskal–Wallis H = 9.046, p = 0.029), with the Sham group showing a significantly greater weight gain (19.00 ± 7.81 g) compared to the DP-MSC group (2.90 ± 15.41 g; p < 0.05; Table 1).

Serum Hormonal Profiles

Biochemical analysis of serum hormone concentrations revealed no statistically significant differences in AMH (p > 0.05) or FSH (p > 0.05) levels among the four experimental groups (Table 2). Serum FSH concentrations were lowest in the Control group (4.68 ± 1.16 mIU/mL) and highest in the POF group (4.99 ± 0.41 mIU/mL). Serum LH concentrations differed significantly among the groups (p = 0.017). Specifically, LH levels were significantly elevated in the untreated POF group (4.90 ± 0.51 mIU/mL) compared with the Sham group (4.04 ± 0.86 mIU/mL; p < 0.05; Table 2), reflecting gonadotropin hypersecretion secondary to chemotherapy-induced ovarian follicular damage.

Ovarian Follicle Dynamics and Morphometry

Histomorphometric follicle counts demonstrated profound alterations in follicular dynamics following CTX administration and substantial recovery following DP-MSC transplantation (Table 3).

The primordial follicle count was significantly decreased in the untreated POF group (10.67 ± 2.18) compared with the Control (19.80 ± 3.90), Sham (24.57 ± 4.72), and DP-MSC (20.00 ± 2.36) groups (p = 0.0001; Table 3).

Evaluation of developing follicles showed that primary follicle numbers were significantly reduced in the POF group (5.56 ± 2.24) relative to the Sham (9.43 ± 2.07) and DP-MSC (10.40 ± 3.75) groups (p = 0.006). Secondary follicle counts were significantly higher in the DP-MSC group (11.00 ± 2.79) than in the POF group (5.78 ± 3.27; p = 0.013). Similarly, tertiary (antral) follicle counts were significantly depleted in the POF group (1.44 ± 1.67) compared with both the Control (6.20 ± 1.92) and DP-MSC (6.60 ±

Table 2: Comparison of serum AMH, FSH, and LH levels in the experimental groups.

		AMH (ng/ml)	FSH (mIU/ml)	LH (mIU/ml)
Control	A.M. ±S.D	4.17±0.6	4.68±1.16	4.13±0.48
	Med (IQR)	4.23 (3.67-4.64)	5.02 (3.7-5.49)	4.15 (3.7-4.56)
	min – max	3.23-4.83	2.69-5.49	3.5-4.79
Sham	A.M. ±S.D	4.12±0.51	4.94±0.33	4.04±0.86
	Med (IQR)	3.86 (3.71-4.59)	4.91 (4.86-5.01)	4.34(3.42-4.81)
	min – max	3.58-4.93	4.43-5.56	2.69-4.93
POF	A.M. ±S.D	4.43±0.3	4.99±0.41	4.9±0.51 (a)
	Med (IQR)	4.34 (4.22-4.68)	5.19 (4.53-5.33)	4.86 (4.48-5.3)
	min – max	3.98-4.97	4.41-5.46	4.11-5.76
DP-MSC	A.M. ±S.D	4.36±0.61	4.69±0.32	4.8±0.53
	Med (IQR)	4.55 (4.13-4.77)	4.72 (4.51-4.92)	4.97 (4.53-5.1)
	min – max	2.81-4.86	4.01-5.19	3.67-5.57
Intergroup p-value		p>0.05	p>0.05	p=0.017*

*p<0.05 A.M: Arithmetic mean, S.D: Standard deviation, Med (IQR): Median (25th-75th percentiles), min – max: Minimum and maximum values, F: One-Way Analysis of Variance, kw: Kruskal-Wallis Analysis of Variance, a: Significant difference versus the Sham group.

3.57) groups (p = 0.001). The number of functional corpora lutea was significantly increased in the DP-MSC group (28.60 ± 5.34) compared with the POF group (20.11 ± 7.41; p = 0.029).

Conversely, the POF group exhibited a marked increase in degenerate structures, demonstrating significantly higher numbers of atretic follicles (13.89 ± 4.01 vs. 3.80 ± 0.84 in Control, 2.71 ± 1.38 in Sham, and 5.50 ± 1.43 in DP-MSC; p = 0.0001) and cystic follicles (7.00 ± 2.55 vs. 2.20 ± 1.10 in Control, 2.29 ± 0.95 in Sham, and 2.50 ± 1.18 in DP-MSC; p = 0.001; Table 3).

Histopathological Findings

Histological evaluation of H&E-stained ovarian sections revealed distinct structural differences among the experimental groups (Figure 2).

In the Control and Sham groups, normal ovarian histoarchitecture was well preserved, featuring an intact single layer of cuboidal surface germinal epithelium, a distinct tunica albuginea, and organized cortical stroma. Follicles across various developmental stages—including primordial, primary, secondary, and tertiary follicles—along with healthy corpora lutea were regularly distributed throughout the cortex.

In contrast, the POF group displayed marked histopathological damage, characterized by severe cortical thinning, interstitial stromal fibrosis, and pronounced depletion of the primordial follicle pool. The developing follicular cohorts were drastically reduced, with a predominance of atretic follicles exhibiting apoptotic granulosa cells, cell detachment from the basement membrane, and distorted oocytes.

In the DP-MSC-treated group, ovarian architecture was notably preserved and restored. The surface epithelium remained intact, the cortical stroma was well organized, and an abundant population of primordial follicles was present. Primary, secondary, and tertiary follicles showed normal multilayered granulosa organization and clear antral spaces, alongside prominent corpora lutea and a substantial reduction in atretic and cystic degenerations (Figure 2).

Immunohistochemical Localization of Wnt-1, Wnt-4, and β-Catenin

Immunohistochemical staining was performed to evaluate the spatial expression and localization of Wnt-1, Wnt-4, and β-catenin in the ovary:

- **Wnt-1:** Strong Wnt-1 immunoreactivity was localized in primordial follicles of the Control, Sham, and DP-MSC groups, whereas staining intensity was noticeably reduced (weak-to-moderate) in primordial follicles of the POF group (Figure 3). Developing follicles (primary, secondary, and tertiary) and corpora lutea displayed positive Wnt-1 staining across all groups, with highest intensity in the corpora lutea of the Control group (Figure 3).

Table 3: Comparison of primordial, primary, secondary, tertiary, atretic, corpus luteum, and cystic follicle numbers in the experimental groups.

		Primordial follicle	Primary follicle	Secondary follicle	Tertiary follicle	Atretic follicle	Corpus Luteum	Cystic Follicle
Control	A.M. ± S.D	19.8 ± 3.9	8.2 ± 1.92	7 ± 4.3	6.2 ± 1.92 (b)	3.8 ± 0.84 (b)	26 ± 4	2.2 ± 1.1 (b)
	Med (IQR)	20 (16.5 - 23)	8 (6.5 - 10)	7 (3.5 - 10.5)	6 (4.5 - 8)	4 (3 - 4.5)	25 (23 - 29.5)	3 (1 - 3)
	min – max	16 - 26	6 - 11	3 - 14	4 - 9	3 - 5	21 - 32	1 - 3
Sham	A.M. ± S.D	24.57 ± 4.72 (b)	9.43 ± 2.07 (b)	7.29 ± 3.4	4 ± 1.83	2.71 ± 1.38 (b)	22.86 ± 5.67	2.29 ± 0.95 (b)
	Med (IQR)	24 (22 - 28)	9 (9 - 10)	7 (5 - 9)	4 (3 - 5)	3 (1 - 4)	23 (17 - 29)	3 (1 - 3)
	min – max	16 - 30	6 - 13	4 - 14	1 - 7	1 - 4	15 - 30	1 - 3
POF	A.M. ± S.D	10.67 ± 2.18 (a,c)	5.56 ± 2.24 (a,c)	5.78 ± 3.27 (a)	1.44 ± 1.67 (a,d)	13.89 ± 4.01 (a,c,d)	20.11 ± 7.41 (a)	7 ± 2.55 (a,c,d)
	Med (IQR)	11 (8 - 13)	6 (4 - 7.5)	5 (3 - 8.5)	1 (0 - 2.5)	13 (10.5 - 17.5)	18 (15.5 - 27)	7 (4.5 - 9.5)
	min – max	8 - 13	1 - 8	2 - 12	0 - 5	10 - 21	9 - 32	3 - 10
DP-MSC	A.M. ± S.D	20 ± 2.36 (b)	10.4 ± 3.75 (b)	11 ± 2.79 (b)	6.6 ± 3.57 (b)	5.5 ± 1.43 (b)	28.6 ± 5.34 (b)	2.5 ± 1.18 (b)
	Med (IQR)	19 (18 - 22.25)	10.5 (7.5 - 12.25)	11 (8.75 - 12.25)	6 (4 - 9.5)	6 (4 - 6.25)	29 (23.5 - 33.5)	2 (2 - 3.25)
	min – max	17 - 24	5 - 18	7 - 17	1 - 13	4 - 8	22 - 37	1 - 5
Intergroup p-value		0.0001* (kw=21.203)	0.006* (F=5.232)	0.013* (F=4.305)	0.001* (F=7.574)	0.0001* (kw=24.314)	0.029* (F=3.511)	0.001* (kw=16.363)

*p<0.05 A.M: Arithmetic mean, S.D: Standard deviation, Med (IQR): Median (25th-75th percentiles), min – max: Minimum and maximum values, F: One-Way Analysis of Variance, kw: Kruskal-Wallis Analysis of Variance, a: Significant difference versus the DP-MSC group; b: Significant difference versus the POF group; c: Significant difference versus the Sham group; d: Significant difference versus the Control Group.

- **Wnt-4:** Wnt-4 immunoreactivity showed striking group- and stage-dependent differences (Figure 4). In primary follicles, strong Wnt-4 staining was detected in the Control, Sham, and DP-MSC groups, but was markedly diminished or absent in the POF group. In secondary follicles, positive staining was maintained across groups, although the POF group showed a distinct linear perioocytic pattern. In tertiary antral follicles, strong cytoplasmic staining was retained across all groups. Furthermore, corpora lutea exhibited strong Wnt-4 expression in the Control, Sham, and DP-MSC groups, compared to only moderate staining in the POF group (Figure 4), confirming that DP-MSC therapy restored Wnt-4 expression.
- **β-Catenin:** β-Catenin staining was consistently positive across all experimental groups (Figure 5). Strong immunoreactivity was observed in oocytes as well as in the cytoplasm and nuclei of granulosa cells within primary, secondary, and tertiary follicles. Robust β-catenin expression was also observed throughout the corpora lutea in all groups (Figure 5).

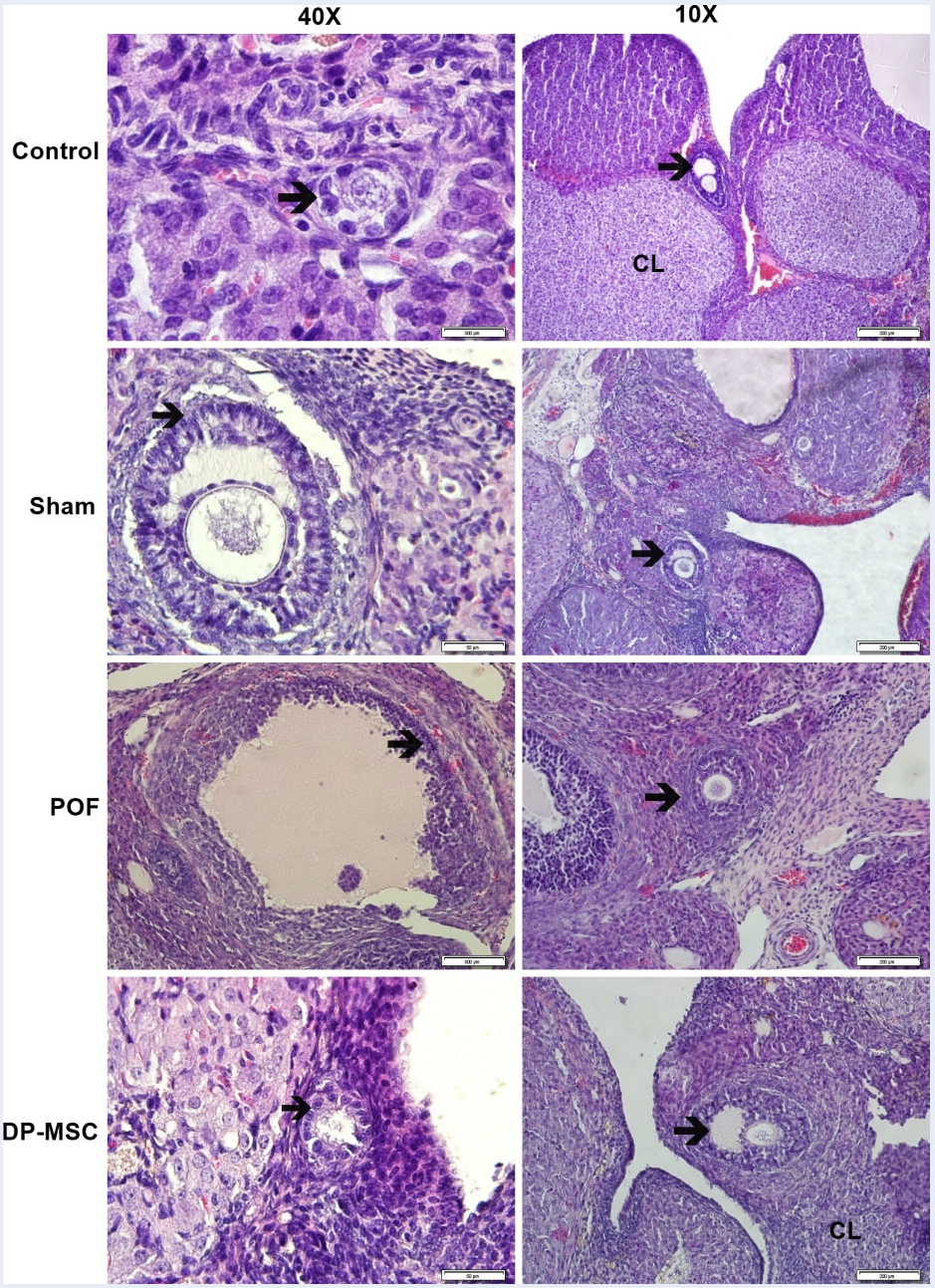

Figure 2: **Histopathological evaluation of ovarian tissue architecture stained with hematoxylin and eosin (H&E) across experimental groups.** Representative photomicrographs of ovarian tissue sections from the Control, Sham, POF (cyclophosphamide-induced), and DP-MSC-treated groups at 400× (40× objective; scale bar = 50 µm) and 100× (10× objective; scale bar = 200 µm) magnification. **Control and Sham groups:** Display normal ovarian histoarchitecture, characterized by an intact, single cuboidal surface germinal epithelium, well-organized cortical stroma, healthy developing follicles at various stages (arrows), and vascularized corpora lutea (CL). **POF group:** Exhibits profound chemotherapy-induced histological deterioration, including marked cortical thinning, stromal vacuolization and fibrosis, loss of primordial follicles, and a high frequency of atretic follicles (arrows) characterized by apoptotic granulosa cell detachment and oocyte degeneration. **DP-MSC group:** Demonstrates remarkable structural restoration following local intraovarian cell transplantation, with preserved surface epithelium, dense cortical stroma, an abundant population of primordial follicles, structurally intact growing follicles (arrows), and healthy corpora lutea (CL), alongside a marked decrease in atretic and cystic degenerations. **Abbreviations:** CL, corpus luteum; DP-MSC, dental pulp–derived mesenchymal stem cell; H&E, hematoxylin and eosin; POF, premature ovarian failure.

DISCUSSION

This study demonstrates that local intraovarian transplantation of human DP-MSCs exerts potent therapeutic and protective effects on ovarian structural architecture and follicular reserve in a cyclophosphamide-induced POF rat model. Chemotherapy with CTX induced severe follicular depletion across all developmental stages, accompanied by extensive stromal fibrosis, increased follicular atresia, and dysregulated serum LH hypersecretion, confirming the successful establishment of ovarian failure. Transplantation of DP-MSCs significantly mitigated these cytotoxic injuries, as evidenced by the restoration of growing follicle cohorts, preservation of the primordial follicle reserve, reduction of atresia and cystic degeneration, and promotion of functional corpus luteum formation. At the molecular level, DP-MSC therapy preserved Wnt-1 expression in primordial follicles and rescued Wnt-4 expression in developing follicles and luteal tissue, while maintaining stable β-catenin localization. Collectively, these findings indicate that DP-MSCs promote ovarian functional and morphological recovery, at least in part, through modulation of the canonical Wnt/β-catenin signaling cascade.

Previous studies have reported that administration of bone marrow–derived MSCs (BM-MSCs) significantly increases body and ovarian weights in experimental POF models[13]. Similarly, human embryonic stem cell–derived MSCs (hESC-MSCs) have been shown to restore body weight and ovarian dimensions following cisplatin-induced gonadotoxicity, thereby improving reproductive outcomes in mice[14]. In contrast, in the present study, while final body weights and net weight gain in the DP-MSC group remained lower than those in non-chemotherapy controls, the animals tolerated local cell delivery well. These findings suggest that, under the current experimental conditions, local intraovarian administration of DP-MSCs primarily exerts localized cytoprotective and reparative actions within the ovarian microenvironment rather than inducing widespread systemic metabolic changes. This localized action is consistent with the well-established paracrine secretome mechanism of MSCs, wherein locally delivered stem cells secrete bioactive cytokines, growth factors, and extracellular vesicles that directly target damaged granulosa cells and resident ovarian stroma, facilitating tissue repair and signaling modulation independently of systemic weight alteration.

The pathogenesis of chemotherapy-induced POF is primarily driven by a dual destructive mechanism: the direct induction of apoptotic cell death in actively proliferating granulosa cells and the accelerated, pathological recruitment of dormant primordial follicles—frequently conceptualized as the "burn-out" phenomenon[15]. Alkylating antineoplastic agents, such as CTX and its active metabolite phosphoramide mustard, trigger abnormal hyperactivation of dormant primordial follicles via the PTEN/PI3K/Akt pathway, causing their mass entry into the growing pool and subsequent rapid apoptotic exhaustion[16,17]. In concordance with this mechanism, previous investigations utilizing CTX or pelvic irradiation reported profound reductions in total follicle counts and extensive follicular atresia[13,18]. Consistent with these reports, our histological data demonstrated extensive depletion across primordial, primary, secondary, and tertiary follicle pools, accompanied by interstitial fibrosis and elevated follicular atresia, confirming the multifaceted ovarian parenchymal damage inflicted by the CTX regimen.

The severity and spatial pattern of ovarian damage are closely governed by the specific chemotherapy administration protocol. For instance, Song et al.[19] reported that repeated low-dose CTX administration primarily depleted secondary follicles with relatively modest effects on other follicular stages. In contrast, the combined regimen utilized in our study—comprising an initial loading dose of 200 mg/kg followed by daily maintenance doses of 8 mg/kg for 14 consecutive days—induced pan-follicular depletion across all developmental stages, accompanied by marked stromal atrophy. This comprehensive ablation of the ovarian reserve establishes a robust, highly reproducible pre-clinical platform to rigorously evaluate stem cell-based regenerative therapies.

Folliculogenesis and ovarian endocrine homeostasis are tightly orchestrated by the hypothalamic–pituitary–gonadal axis, wherein FSH drives granulosa cell proliferation and antral development[20], while AMH, produced by pre-antral and small antral follicles, serves as a surrogate clinical marker of the ovarian primordial reserve[21]. In our study, serum LH concentrations were significantly elevated in the untreated POF group compared with the Sham group, reflecting the loss of negative steroid feedback from depleted follicles. Although DP-MSC administration exhibited a clear trend toward normalizing LH levels, statistically significant differences in serum FSH and AMH were not yet detectable at the 10-day post-transplantation endpoint. This

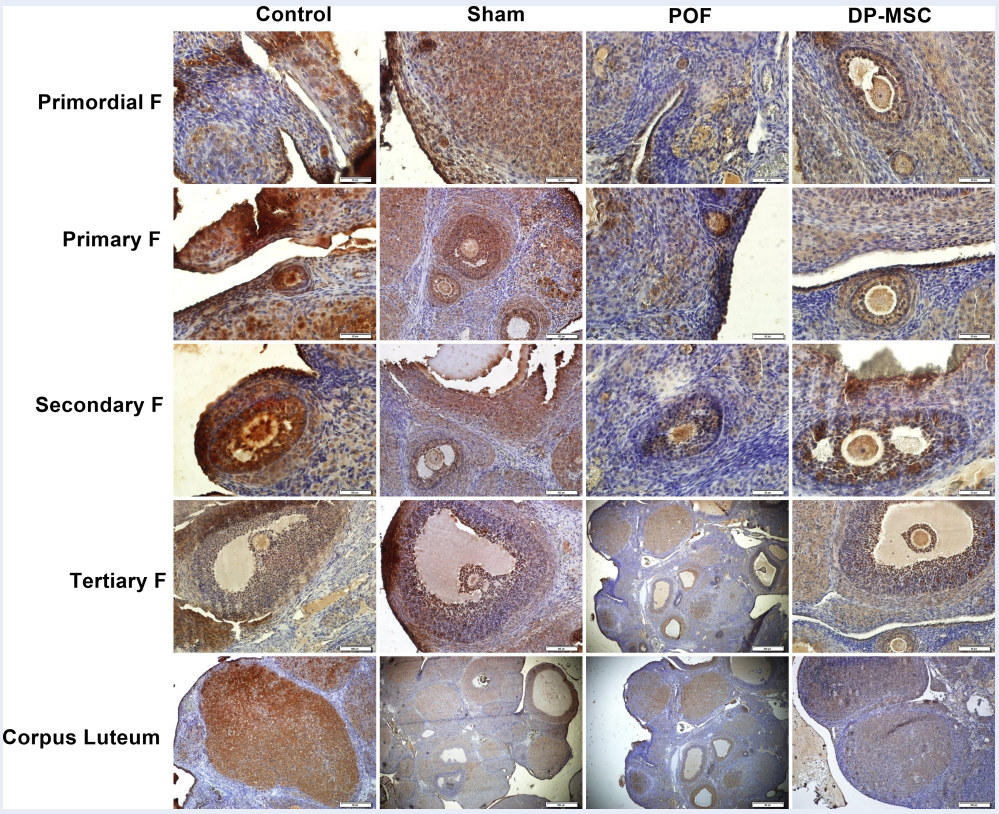

Figure 3: **Immunohistochemical localization and expression of Wnt-1 across ovarian follicular compartments and corpora lutea in experimental groups.** Representative photomicrographs demonstrating Wnt-1 immunoreactivity in primordial follicles (Primordial F), primary follicles (Primary F), secondary follicles (Secondary F), tertiary antral follicles (Tertiary F), and corpora lutea across the Control, Sham, POF, and DP-MSC groups. Immunohistochemical staining was visualized using 3,3′-diaminobenzidine (DAB) chromogen (brown precipitate) with Mayer's hematoxylin counterstaining (blue nuclei). Primordial follicles in the Control, Sham, and DP-MSC groups demonstrate strong positive Wnt-1 immunoreactivity, whereas primordial follicles in the POF group show noticeably attenuated, weak-to-moderate staining. Developing follicles (primary, secondary, and tertiary) and luteal cells of the corpus luteum display positive immunoreactivity across all groups, with the highest staining intensity observed in the corpora lutea of the Control group. Images were captured using a light microscope at 400× magnification (40× objective); scale bar = 50 µm. **Abbreviations:** DAB (3,3′-diaminobenzidine); DP-MSC, dental pulp–derived mesenchymal stem cell; F, follicle; POF, premature ovarian failure; Wnt-1, Wingless-type MMTV integration site family member 1.

observation suggests that functional endocrine recovery may lag behind early histological and morphological reconstitution. Re-establishment of coordinated steroidogenic enzyme expression and systemic feedback loops typically requires a longer post-transplantation maturation window, even after cellular architecture and follicular structures have been substantially restored.

The therapeutic efficacy of diverse MSC populations in animal models of ovarian insufficiency is well established. BM-MSCs have been shown to enhance follicular survival and normalize endocrine parameters[13], whereas human embryonic stem cell–derived and amnion-derived MSCs attenuate apoptotic cascades and enhance granulosa cell viability via paracrine pathways[14,22]. Similarly, umbilical cord–derived MSCs restore folliculogenesis and ovarian vascularization[19]. In alignment with these reports, our findings demonstrated that human DP-MSC transplantation significantly improved ovarian histoarchitecture, increased developing follicle numbers, and suppressed follicular atresia. Importantly, the significantly higher primordial follicle count in the DP-MSC-treated group should not be construed as de novo neo-oogenesis. Because CTX administration was completed prior to cell transplantation, DP-MSCs likely rescued the residual quiescent primordial follicle pool from sec-

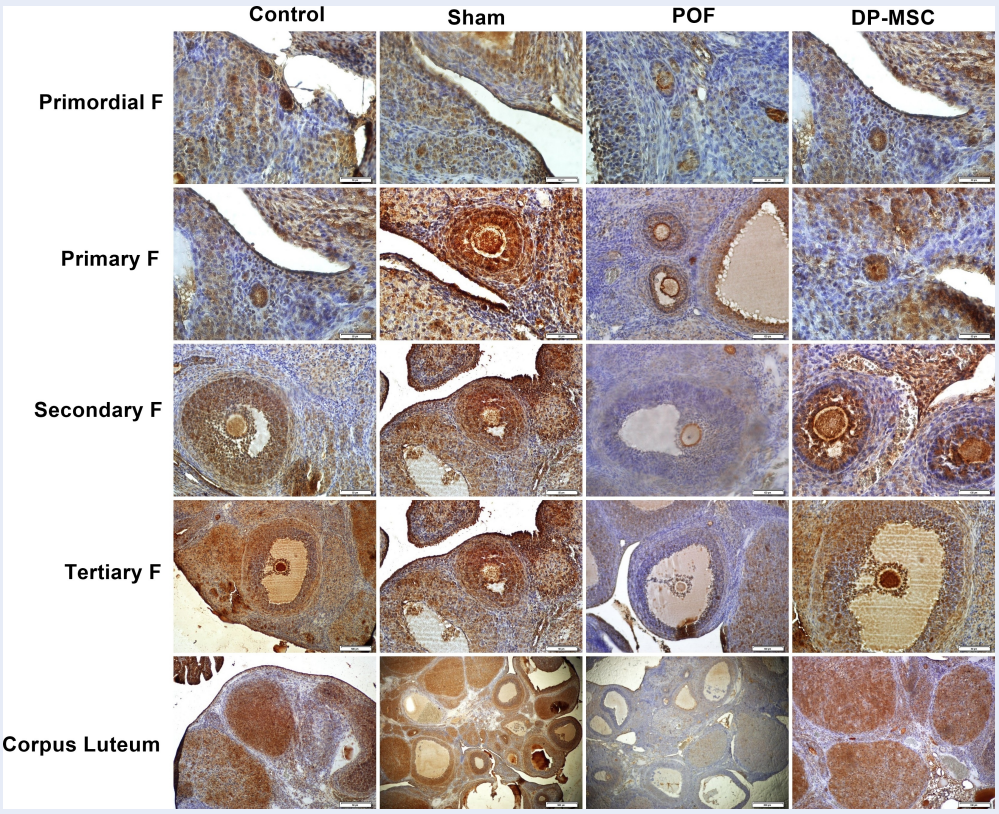

Figure 4: Immunohistochemical localization and rescue of Wnt-4 expression following DP-MSC transplantation in cyclophosphamide-induced POF rats. Representative photomicrographs showing Wnt-4 immunoreactivity across sequential follicular developmental stages (primordial, primary, secondary, and tertiary follicles) and corpora lutea in the Control, Sham, POF, and DP-MSC groups. Specific brown immunoreactivity was developed using DAB substrate counterstained with hematoxylin. Primary follicles in the Control, Sham, and DP-MSC groups show intense Wnt-4 staining, whereas primary follicles in the POF group exhibit markedly depleted or absent staining. Secondary follicles maintain positive expression across all groups, with the POF group showing a distinct linear perioocytic pattern. In tertiary antral follicles, strong cytoplasmic Wnt-4 staining is preserved across all groups. Corpora lutea display moderate staining in the POF group and intense staining in the Control, Sham, and DP-MSC groups, demonstrating that DP-MSC transplantation effectively restores Wnt-4 expression in damaged ovarian parenchyma. Images were acquired at 400× magnification (40× objective); scale bar = 50 μm. **Abbreviations:** DAB (3,3⊠-diaminobenzidine); DP-MSC, dental pulp–derived mesenchymal stem cell; F, follicle; POF, premature ovarian failure; Wnt-4, Wingless-type MMTV integration site family member 4.

ondary, post-chemotherapy apoptotic waves, oxidative stress, and progressive stromal fibrosis. Thus, DP-MSCs act primarily as a cytoprotective and antiatretic rescue agent, offering an accessible, noncontroversial, and highly proliferative alternative cell source for ovarian regenerative medicine.

The canonical Wnt/β-catenin signaling cascade plays an indispensable role in ovarian steroidogenesis, granulosa cell proliferation, and early folliculogenesis in coordination with gonadotropin signaling [10,23]. Intracellular β-catenin functions as the central transcriptional co-activator of this pathway, promoting granulosa cell survival and inhibiting apoptosis. In the present study, β-catenin expression was detected in oocytes and granulosa cells across all experimental groups, including the POF group. While previous studies have reported decreased β-catenin levels in chemotherapy-damaged ovaries [18] or marked upregulation following BM-MSC therapy [13], our immunohistochemical findings revealed a relatively stable baseline distribution. This persistence suggests that β-catenin expression alone is insufficient to maintain follicular integrity in the absence of upstream ligands, and that its activation state and subcellular localization are tightly regulated in a context-dependent manner during ovarian injury and repair.

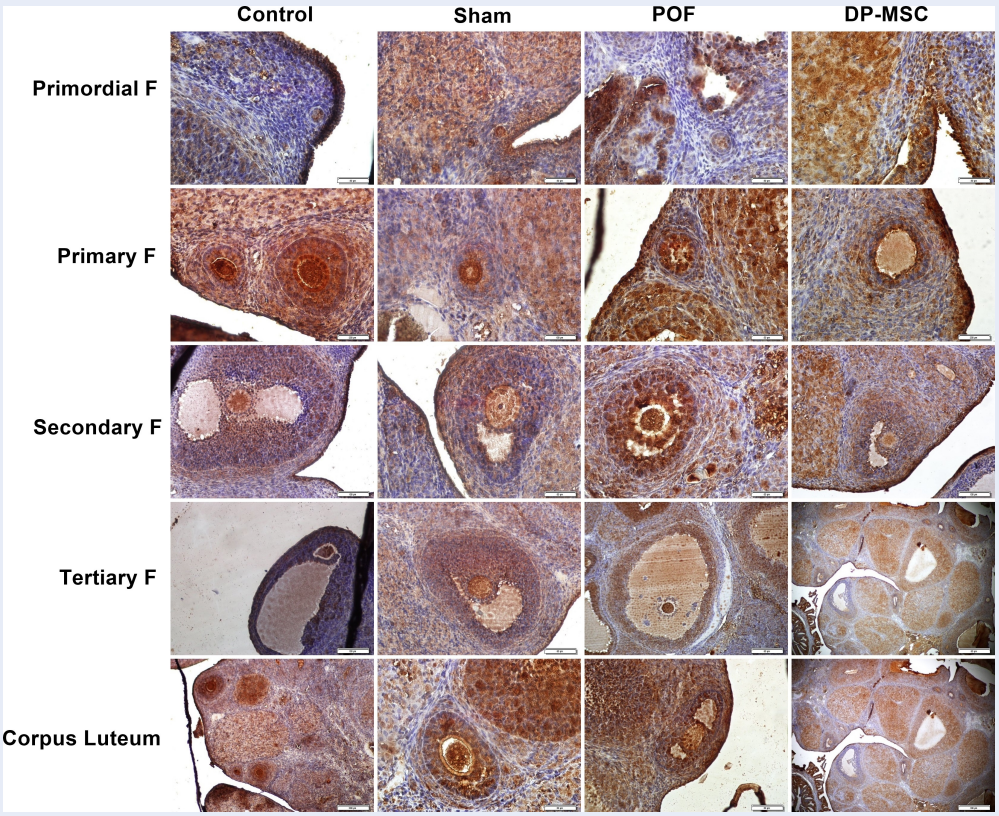

Figure 5: **Immunohistochemical localization of β-catenin across ovarian follicular stages and corpora lutea in experimental groups.** Representative photomicrographs showing β-catenin immunoreactivity in primordial, primary, secondary, and tertiary follicles, as well as corpora lutea, across the Control, Sham, POF, and DP-MSC groups. Brown DAB precipitate indicates specific β-catenin localization counterstained with hematoxylin. Strong β-catenin expression is consistently observed across all experimental groups, localized within oocytes as well as the cytoplasm and nuclei of granulosa cells in primary, secondary, and tertiary follicles. Robust luteal parenchymal staining is also maintained in the corpora lutea of all groups, reflecting active and stable baseline expression of the canonical Wnt transcriptional co-activator. Images were acquired at 400× magnification (40× objective); scale bar = 50 µm. **Abbreviations:** DAB (3,3⊠-diaminobenzidine); DP-MSC, dental pulp–derived mesenchymal stem cell; F, follicle; POF, premature ovarian failure; β-catenin, beta-catenin.

A pivotal finding of the present investigation was the dynamic modulation of Wnt-4 expression. Wnt-4 is a critical morphogen required for female sexual differentiation, pre-antral and antral follicle growth, steroidogenesis, and luteal function[24,25]. Targeted deletion of Wnt-4 severely compromises follicular maturation and leads to female infertility[9]. Although Wnt-4 is expressed dynamically across follicular stages in rodents, its detection in human granulosa cells varies, reflecting potential species-specific regulatory mechanisms[26–28]. In our study, CTX-induced ovarian failure was accompanied by a marked loss of Wnt-4 immunoreactivity in primary follicles and corpora lutea, whereas DP-MSC transplantation robustly restored Wnt-4 expression in developing follicles and luteal tissue. Concurrently, Wnt-1 expression in primordial follicles was preserved following DP-MSC treatment. Together with the stable baseline of β-catenin, these findings suggest that DP-MSCs promote follicular rescue and development by reactivating upstream canonical and potentially non-canonical Wnt ligands.

The biological consequences of Wnt signaling activation are inherently context-dependent, balancing tissue regeneration against pathological fibrosis. Aberrant, uncontrolled hyperactivation of canonical Wnt/β-catenin signaling has been implicated in pathological myofibroblast differentiation and organ fibrosis[29]. Furthermore, environmental toxicant exposure, such as microplastic ingestion, has been shown to overactivate Wnt/β-catenin signaling, triggering granulosa cell apoptosis, oxidative stress,

and ovarian fibrosis[30]. In this context, the persistent basal β-catenin expression observed in the POF group may reflect a dual biological phenomenon: a compensatory mechanism to support residual follicular survival alongside concurrent pathological stromal remodeling.

Several limitations of this study should be acknowledged. First, although DP-MSC transplantation demonstrated clear histological and morphological benefits, long-term functional reproductive outcomes—including estrous cyclicity, mating success, ovulation rates, and live birth rates—were not evaluated. Second, while immunohistochemical assessments demonstrated spatial localization and intensity alterations of Wnt-1, Wnt-4, and β-catenin, quantitative molecular methodologies, such as quantitative real-time PCR (RT-qPCR) and Western blotting, are needed to elucidate downstream transcriptional targets. Third, immunohistochemical evaluation relied on semi-quantitative grading rather than automated digital image morphometry. Future investigations incorporating digital image analysis and molecular pathway inhibition will be instrumental in fully elucidating the paracrine mechanisms and clinical translational potential of DP-MSCs in ovarian rejuvenation.

CONCLUSION

In conclusion, local intraovarian transplantation of human DP-MSCs effectively preserves the follicular reserve and restores ovarian histological architecture in a rat model of cyclophosphamide-induced premature ovarian failure. These therapeutic effects are mediated, at least in part, through modulation of the canonical Wnt/β-catenin signaling cascade, specifically via the preservation of Wnt-1 and the reactivation of Wnt-4 expression in follicular and luteal compartments. These findings position DP-MSCs as a promising, readily accessible, and biologically potent cell-based therapeutic candidate for counteracting chemotherapy-induced gonadotoxicity and promoting ovarian tissue regeneration.

ABBREVIATIONS

AMH: Anti-Müllerian hormone; ANOVA: Analysis of variance; BM-MSCs: Bone marrow–derived mesenchymal stem cells; CTX: Cyclophosphamide; DAB: 3,3′-Diaminobenzidine; DMEM: Dulbecco's Modified Eagle Medium; DP-MSCs: Dental pulp–derived mesenchymal stem cells; ELISA: Enzyme-linked immunosorbent assay; FBS: Fetal bovine serum; FSH: Follicle-stimulating hormone; H&E: Hematoxylin and eosin; hESC-MSCs: Human embryonic stem cell–derived mesenchymal stem cells; HRP: Horseradish peroxidase; IQR: Interquartile range; LH: Luteinizing hormone; MSCs: Mesenchymal stem cells; PBS: Phosphate-buffered saline; POF: Premature ovarian failure; POI: Primary ovarian insufficiency; RT-qPCR: Quantitative real-time polymerase chain reaction; SD: Standard deviation; Wnt: Wingless-related integration site.

ACKNOWLEDGMENTS

The authors thank the Pamukkale University Scientific Research Projects Coordination Unit for financial and administrative support (Project number: 2021SABE023).

AUTHOR'S CONTRIBUTIONS

Funding acquisition: NÇ, MŞ; Conception: NÇ, MŞ; Methodology: NÇ, MŞ, CK, HŞ, EM, GAM; Investigation and data acquisition: NÇ, MŞ, HŞ; Formal analysis and interpretation of data: NÇ, MŞ, HŞ; Writing – original draft preparation: NÇ, MŞ, CK, HŞ, EM, GAM; Writing – review & editing: CK, GAM; Supervision: CK, GAM. All authors read and approved the final manuscript.

FUNDING

This study was supported by the Pamukkale University Scientific Research Projects Coordination Unit through Project number 2021SABE023.

AVAILABILITY OF DATA AND MATERIALS

All processed data and materials supporting the conclusions of this article are included within the manuscript. Additional raw datasets are available from the corresponding author upon reasonable request.

ETHICS APPROVAL AND CONSENT TO PARTICIPATE

All animal experimental procedures were approved by the Pamukkale University Animal Experiments Ethics Committee (Approval No. PAUHDEK-2021/38). Human dental pulp tissue collection was approved by the Pamukkale University Non-Interventional Clinical Research Ethics Committee (Approval No. 17, dated 08 July 2020), and written informed consent was obtained from all tissue donors prior to tooth extraction.

CONSENT FOR PUBLICATION

Not applicable.

DECLARATION OF GENERATIVE AI AND AI-ASSISTED TECHNOLOGIES IN THE WRITING PROCESS

The authors declare that generative artificial intelligence (AI) and AI-assisted technologies were not used in the writing or production of this manuscript. The authors take full responsibility for the content, originality, and integrity of the work.

COMPETING INTERESTS

The authors declare that they have no competing interests.

REFERENCES

1. Wesevich V, Kellen AN, Pal L. Recent advances in understanding primary ovarian insufficiency. F1000Research. 2020;9:F1000 Faculty Rev–1101. PMID: 32934798. Available from: https://doi.org/10.12688/f1000research.26423.1.
2. Liu T, Li Q, Wang S, Chen C, Zheng J. Transplantation of ovarian granulosa-like cells derived from human induced pluripotent stem cells for the treatment of murine premature ovarian failure. Molecular Medicine Reports. 2016;13(6):5053–5058. PMID: 27121006. Available from: https://doi.org/10.3892/mmr.2016.5191.
3. Fu YX, Ji J, Shan F, Li J, Hu R. Human mesenchymal stem cell treatment of premature ovarian failure: new challenges and opportunities. Stem Cell Research & Therapy. 2021;12(1):161. PMID: 33658073. Available from: https://doi.org/10.1186/s13287-021-02212-0.
4. Spangrude GJ. When is a stem cell really a stem cell? Bone Marrow Transplantation. 2003;32(Suppl 1):S7–S11. PMID: 12931232. Available from: https://doi.org/10.1038/sj.bmt.1703936.
5. Lorzadeh N, Kazemirad N. Application of stem cells to infertility treatment with emphasis on mesenchymal stem cells and ovarian stem cells. American Journal of Perinatology. 2018;35(12):1142–1147. PMID: 29715701. Available from: https://doi.org/10.1055/s-0038-1646948.
6. Tsutsui TW. Dental pulp stem cells: advances to applications. Stem Cells and Cloning: Advances and Applications. 2020;13:33–42. PMID: 32104005. Available from: https://doi.org/10.2147/SCCAA.S166759.
7. Shi X, Mao J, Liu Y. Pulp stem cells derived from human permanent and deciduous teeth: biological characteristics and therapeutic applications. Stem Cells Translational Medicine. 2020;9(4):445–464. PMID: 31943813. Available from: https://doi.org/10.1002/sctm.19-0398.
8. Castagnoli L, Tagliabue E, Pupa SM. Inhibition of the Wnt signalling pathway: an avenue to control breast cancer aggressiveness. International Journal of Molecular Sciences. 2020;21(23):9069. PMID: 33260642. Available from: https://doi.org/10.3390/ijms21239069.
9. Naillat F, Yan W, Karjalainen R, Liakhovitskaia A, Samoylenko A, Xu Q, et al. Identification of the genes regulated by Wnt-4, a critical signal for commitment of the ovary. Experimental Cell Research. 2015;332(2):163–178. PMID: 25645944. Available from: https://doi.org/10.1016/j.yexcr.2015.01.010.
10. Parakh TN, Hernandez JA, Grammer JC, Weck J, Hunzicker-Dunn M, Zeleznik AJ, et al. Follicle-stimulating hormone/cAMP regulation of aromatase gene expression requires beta-catenin. Proceedings of the National Academy of Sciences of the United States of America. 2006;103(33):12435–12440. PMID: 16895991. Available from: https://doi.org/10.1073/pnas.0603006103.
11. Çil N, Mete GA. The effect of adipose-derived mesenchymal stem cell treatment on mTOR and p-mTOR expression in ovarian damage due to cyclophosphamide. Reproductive Toxicology. 2021;103:71–78. PMID: 34098046. Available from: https://doi.org/10.1016/j.reprotox.2021.06.003.
12. Mayer LP, Pearsall NA, Christian PJ, Devine PJ, Payne CM, McCuskey MK, et al. Long-term effects of ovarian follicular depletion in rats by 4-vinylcyclohexene diepoxide. Reproductive Toxicology. 2002;16(6):775–781. PMID: 12401505. Available from: https://doi.org/10.1016/s0890-6238(02)00048-5.
13. El-Derany MO, Said RS, El-Demerdash E. Bone marrow-derived mesenchymal stem cells reverse radiotherapy-induced premature ovarian failure: emphasis on signal integration of TGF-β, Wnt/β-catenin and Hippo pathways. Stem Cell Reviews and Reports. 2021;17(4):1429–1445. PMID: 33594662. Available from: https://doi.org/10.1007/s12015-021-10135-9.
14. Yoon SY, Yoon JA, Park M, Shin EY, Jung S, Lee JE, et al. Recovery of ovarian function by human embryonic stem cell-derived mesenchymal stem cells in cisplatin-induced premature ovarian failure in mice. Stem Cell Research & Therapy. 2020;11(1):255. PMID: 32586410. Available from: https://doi.org/10.1186/s13287-020-01769-6.
15. Kalich-Philosoph L, Roness H, Carmely A, Fishel-Bartal M, Ligumsky H, Paglin S, et al. Cyclophosphamide triggers follicle activation and "burnout"; AS101 prevents follicle loss and preserves fertility. Science Translational Medicine. 2013;5(185):185ra62. PMID: 23677591. Available from: https://doi.org/10.1126/scitranslmed.3005402.
16. Jang H, Lee OH, Lee Y, Yoon H, Chang EM, Park M, et al. Melatonin prevents cisplatin-induced primordial follicle loss via suppression of PTEN/AKT/FOXO3a pathway activation in the mouse ovary. Journal of Pineal Research. 2016;60(3):336–347. PMID: 26882203. Available from: https://doi.org/10.1111/jpi.12316.
17. Chang EM, Lim E, Yoon S, Jeong K, Bae S, Lee DR, et al. Cisplatin induces overactivation of the dormant primordial follicle through PTEN/AKT/FOXO3a pathway which leads to loss of ovarian reserve in mice. PLoS One. 2015;10(12):e0144245. PMID: 26656301. Available from: https://doi.org/10.1371/journal.pone.0144245.
18. Chen C, Li S, Hu C, Cao W, Fu Q, Li J, et al. Protective effects of puerarin on premature ovarian failure via regulation of Wnt/β-catenin signaling pathway and oxidative stress. Reproductive Sciences. 2021;28(4):982–990. PMID: 32996063. Available from: https://doi.org/10.1007/s43032-020-00325-0.
19. Song D, Zhong Y, Qian C, Zou Q, Ou J, Shi Y, et al. Human umbilical cord mesenchymal stem cells therapy in cyclophosphamide-induced premature ovarian failure rat model. BioMed Research International. 2016;2016:2517514. PMID: 27047962. Available from: https://doi.org/10.1155/2016/2517514.
20. Gharib SD, Wierman ME, Shupnik MA, Chin WW. Molecular biology of the pituitary gonadotropins. Endocrine Reviews. 1990;11(1):177–199. PMID: 2108012. Available from: https://doi.org/10.1210/edrv-11-1-177.
21. van Rooij IA, Broekmans FJ, te Velde ER, Fauser BC, Bancsi LF, de Jong FH, et al. Serum anti-Müllerian hormone levels: a novel measure of ovarian reserve. Human Reproduction. 2002;17(12):3065–3071. PMID: 12456604. Available from: https://doi.org/10.1093/humrep/17.12.3065.
22. Ling L, Feng X, Wei T, Wang Y, Wang Y, Wang Z, et al. Human amnion-derived mesenchymal stem cell (hAD-MSC) transplantation improves ovarian function in rats with premature ovarian insufficiency (POI) at least partly through a paracrine mechanism. Stem Cell Research & Therapy. 2019;10(1):46. PMID: 30683144. Available from: https://doi.org/10.1186/s13287-019-1136-x.
23. Fan HY, O'Connor A, Shitanaka M, Shimada M, Liu Z, Richards JS. Beta-catenin (CTNNB1) promotes preovulatory follicular development but represses LH-mediated ovulation and luteinization. Molecular Endocrinology. 2010;24(8):1529–

1542. PMID: 20610534. Available from: https://doi.org/10.1210/me.2010-0141.

24. Boyer A, Goff AK, Boerboom D. WNT signaling in ovarian follicle biology and tumorigenesis. Trends in Endocrinology and Metabolism. 2010;21(1):25–32. PMID: 19875303. Available from: https://doi.org/10.1016/j.tem.2009.08.005.
25. Boyer A, Lapointe E, Zheng X, Cowan RG, Li H, Quirk SM, et al. WNT4 is required for normal ovarian follicle development and female fertility. FASEB Journal. 2010;24(8):3010–3025. PMID: 20371632. Available from: https://doi.org/10.1096/fj.09-145789.
26. Hsieh M, Johnson MA, Greenberg NM, Richards JS. Regulated expression of Wnts and Frizzleds at specific stages of follicular development in the rodent ovary. Endocrinology. 2002;143(3):898–908. PMID: 11861511. Available from: https://doi.org/10.1210/endo.143.3.8684.
27. Hernandez-Gonzalez I, Gonzalez-Robayna I, Shimada M, Wayne CM, Ochsner SA, White L, et al. Gene expression profiles of cumulus cell oocyte complexes during ovulation reveal cumulus cells express neuronal and immune-related genes: does this expand their role in the ovulation process? Molecular Endocrinology. 2006;20(6):1300–1321. PMID: 16455817. Available from: https://doi.org/10.1210/me.2005-0420.
28. Wang HX, Tekpetey FR, Kidder GM. Identification of WNT/beta-CATENIN signaling pathway components in human cumulus cells. Molecular Human Reproduction. 2009;15(1):11–17. PMID: 19038973. Available from: https://doi.org/10.1093/molehr/gan070.
29. Huang GR, Wei SJ, Huang YQ, Xing W, Wang LY, Liang LL. Mechanism of combined use of vitamin D and puerarin in anti-hepatic fibrosis by regulating the Wnt/β-catenin signalling pathway. World Journal of Gastroenterology. 2018;24(36):4178–4185. PMID: 30271082. Available from: https://doi.org/10.3748/wjg.v24.i36.4178.
30. An R, Wang X, Yang L, Zhang J, Wang N, Xu F, et al. Polystyrene microplastics cause granulosa cells apoptosis and fibrosis in ovary through oxidative stress in rats. Toxicology. 2021;449:152665. PMID: 33359712. Available from: https://doi.org/10.1016/j.tox.2020.152665.